Infrared absorption of gaseous ClCS detected with time-resolved Fourier-transform spectroscopy

Li-Kang Chu, Hui-Ling Han, and Yuan-Pern Lee

Citation: The Journal of Chemical Physics **126**, 174310 (2007); doi: 10.1063/1.2730501
View online: http://dx.doi.org/10.1063/1.2730501
View Table of Contents: http://scitation.aip.org/content/aip/journal/jcp/126/17?ver=pdfcov
Published by the AIP Publishing

Infrared absorption of gaseous ClCS detected with time-resolved Fourier-transform spectroscopy

Li-Kang Chu and Hui-Ling Han
Department of Applied Chemistry, National Chiao Tung University, 1001 Ta-Hsueh Road, Hsinchu 30010, Taiwan and Institute of Molecular Science, National Chiao Tung University, 1001 Ta-Hsueh Road, Hsinchu 30010, Taiwan

Yuan-Pern Lee[a)]
Department of Applied Chemistry, National Chiao Tung University, 1001 Ta-Hsueh Road, Hsinchu 30010, Taiwan; Institute of Molecular Science, National Chiao Tung University, 1001 Ta-Hsueh Road, Hsinchu 30010, Taiwan; and Institute of Atomic and Molecular Sciences, Academia Sinica, Taipei 10617, Taiwan

(Received 6 March 2007; accepted 21 March 2007; published online 7 May 2007)

A transient infrared absorption spectrum of gaseous ClCS was detected with a step-scan Fourier-transform spectrometer coupled with a multipass absorption cell. ClCS was produced upon irradiating a flowing mixture of Cl_2CS and N_2 or CO_2 with a KrF excimer laser at 248 nm. A transient band in the region of 1160–1220 cm^{-1}, which diminished on prolonged reaction, is assigned to the C–S stretching (ν_1) mode of ClCS. Calculations with density-functional theory (B3P86 and B3LYP/aug-cc-pVTZ) predict the geometry, vibrational wave numbers, and rotational parameters of ClCS. The rotational contour of the spectrum of ClCS simulated based on predicted rotational parameters agrees satisfactorily with experimental observation; from spectral simulation, the band origin is determined to be at 1194.4 cm^{-1}. Reaction kinetics involving ClCS, CS, and CS_2 are discussed. © *2007 American Institute of Physics*. [DOI: 10.1063/1.2730501]

I. INTRODUCTION

Thiocarbonyls and carbonyls exhibit qualitatively similar bonding, but their photochemistry and photophysics differ substantially.[1–5] For example, for larger thiocarbonyls, their lower excited states are typically more photostable and tend to relax by photophysical rather than photochemical processes.[3] Thiophosgene (or thiocarbonyl chloride, Cl_2CS), as one of the simplest halogen-substituted thiocarbonyls, has had extensive experimental[6–14] and theoretical[7,15–18] investigations. Cl_2CS absorbs weakly in the visible region to produce the lowest triplet (T_1) and lowest singlet (S_1) excited states, which correspond to symmetry-forbidden $n \rightarrow \pi^*$ transitions[3] with band origins at 17 492 and 18 716 cm^{-1}, respectively; the symbol * indicates antibonding orbitals. The second singlet excited state (S_2), corresponding to a $\pi \rightarrow \pi^*$ excitation, lies ~34 275 cm^{-1} above the ground electronic state. Fluorescence from the S_2 state diminishes when the excitation energy is ~1450 cm^{-1} above the vibrational ground level because of predissociation.[11,12]

Three major channels for ultraviolet photodissociation of Cl_2CS are expected,

$$Cl_2CS \rightarrow ClCS + Cl, \quad \Delta H^0 = 265 \text{ kJ mol}^{-1}, \tag{1}$$

$$Cl_2CS \rightarrow Cl_2 + CS, \quad \Delta H^0 = 240 \text{ kJ mol}^{-1}, \tag{2}$$

$$Cl_2CS \rightarrow 2\,Cl + CS, \quad \Delta H^0 = 479 \text{ kJ mol}^{-1}, \tag{3}$$

in which experimental enthalpies of reaction are derived from enthalpies of formation (in kJ mol^{-1}) at 0 K as follows: Cl: 119.6,[19] CS: 275±4,[20] ClCS: 180±4,[6] and Cl_2CS: 35±4; the value for Cl_2CS was derived based on the bond energy D_0 (SClC–Cl) of 265±4 kJ mol^{-1} (Ref. 6) and the enthalpies of formation of Cl and ClCS. Previous theoretical calculations by Hachey *et al.* showed $\Delta H = 238$ kJ mol^{-1} and $\Delta H = 477$ kJ mol^{-1} for reactions (2) and (3), respectively, and a barrier of ~299 kJ mol^{-1} for reaction (2).[21]

Photolysis at 248 nm (~482 kJ mol^{-1}) of Cl_2CS in a pulsed molecular beam yields Cl_2 and ClCS, indicating the existence of channels (1) and (2); the branching ratio for reaction (1) was determined to be 0.8±0.1.[13] The photodissociation dynamics at 235 nm were investigated with detection of Cl ($^2P_{3/2}$) and Cl^* ($^2P_{1/2}$) by time-of-flight resonance-enhanced multiphoton ionization.[14] The counter product, ClCS, was formed mostly in electronically excited states $A\,^2A''$ and $B\,^2A'$; the percentage proportions of *X*, *A*, and *B* states of ClCS are 4:60:36 and 7.5:71.5:21 for associated atomic fragments Cl and Cl^*, respectively. The photophysics and photochemistry of Cl_2CS have been investigated with quantum-chemical calculations on the potential-energy surfaces for dissociation of Cl_2CS into ClCS+Cl in the first five excited electronic states according to a combined complete active space self-consistent field and multireference configuration interaction method.[18] Upon irradiation in the range of 235–253 nm Cl_2CS is excited to its S_2 state, followed by direct dissociation to ClCS (*A*) and Cl ($^2P_{3/2}$). Although experimental investigations on photodissociation dynamics of

[a)]Author to whom correspondence should be addressed. Fax: 886-3-5713491. Electronic mail: yplee@mail.nctu.edu.tw

Cl_2CS involve mass spectrometry to probe ClCS, no direct spectral detection of gaseous ClCS has been previously reported.

Schallmoser *et al.* produced ClCS with a pulsed discharge jet of Cl_2CS/Ar, $CS_2/Cl_2/Ar$, $CS_2/CCl_4/Ar$, and their isotopic variants, and deposited the gaseous mixture onto a cold substrate; they observed absorption lines at 1189.3 and 632.1 cm^{-1} which they attributed to the ν_1 (C–S stretching) and ν_3 (C–Cl stretching) modes of ClCS isolated in solid Ar.[22] Chan and Goddard predicted geometries, vibrational wave numbers, and energies of ClCS in the ground ($X\,^2A'$) and first electronically excited states ($A\,^2A''$) using restricted singles-and-doubles configuration-interaction (RCISD/6-31G*) methods.[23] Vibrational wave numbers of the $X\,^2A''$ state of ClCS are predicted to be $\nu_1=1314$ cm^{-1}, ν_2 (ClCS bend)$=355$ cm^{-1}, and $\nu_3=699$ cm^{-1}; these values differ by more than 10% from the values observed in matrix experiments.[22]

It is of interest to develop an infrared (IR) detection technique to investigate further the photodissociation dynamics of Cl_2CS and reaction kinetics involving ClCS. We have successfully coupled a step-scan Fourier-transform spectrometer with a multipass absorption cell to record time-resolved infrared absorption spectra of reaction intermediates in the gaseous phase.[24–27] Here we report an application of this technique to record transient IR absorption spectra of the intermediate ClCS upon photodissociation of Cl_2CS.

II. EXPERIMENTS

A commercial step-scan spectrometer (Thermo Nicolet, Nexus 870) was employed for transient absorption measurements.[26,27] A White cell with an effective path length of 6.4 m (base path of 20 cm) and a volume of ~2000 cm^3 served as the reactor and was placed in the sample compartment of the Fourier transform infrared (FTIR) spectrometer. Two rectangular (3×12 cm^2) quartz windows on the sides of the White cell allow passage of the photolysis laser beam that propagates perpendicular to the multipassing IR beam. The laser beam is multiply reflected between a pair of external rectangular laser mirrors and passes these quartz windows and the White cell after each reflection. A KrF excimer laser (GAM Laser, EX100H/60) operated at 8 Hz with typical output energy of ~80 mJ $pulse^{-1}$ at 248 nm and a beam expanded by a telescope to a dimension $\sim4\times1.5$ cm^2 was employed for photodissociation. The ac-coupled signal from the fast mercury cadmium telluride (20 MHz) detector was further amplified (Stanford Research Systems, Model SR560) 20 times with a bandwidth 0.1–1000 kHz before being sent to the external 14 bit digitizer (Gage Applied Technology, CompuScope 14100, 10^8 samples s^{-1}), whereas the dc-coupled signal was sent directly to the internal 16 bit digitizer (2×10^5 samples s^{-1}) of the spectrometer. Techniques for obtaining time-resolved difference absorption spectra with a step-scan FTIR spectrometer are well established.[24,28] The position of the moving mirror of FTIR was maintained to within ±0.2 nm at each step in the step-scan mode.[29]

Typically, 300 data points were acquired at 0.2 μs integrated intervals (20 dwells at 10 ns gate width) after each laser shot; the signal was typically averaged over 25 laser shots at each scan step. We utilized undersampling by employing appropriate optical filters to define a small spectral region to decrease the number of points in the interferogram, hence the duration of data acquisition. For spectra in the range of 900–1700 cm^{-1} at a resolution of 4 cm^{-1}, 552 scan steps were required, and the data acquisition lasted ~40 min. For the spectral range 910–1350 cm^{-1} at a resolution of 0.6 cm^{-1}, 1656 scan steps were required, and the data acquisition lasted ~80 min; in this case, the laser was triggered at 10 Hz and 16 acquisitions were averaged for each scan step. To improve further the ratio of signal to noise, we recorded and averaged four sets of data under similar experimental conditions.

A flowing mixture of Cl_2CS/N_2 or Cl_2CS/CO_2 with flow rates $F_{Cl_2CS}=0.18$–0.22 cm^3 s^{-1}, $F_{N_2}\cong29.1$ cm^3 s^{-1} or $F_{CO_2}\cong14.4$ cm^3 s^{-1} at STP, and total pressure $P_T\cong43$–52 Torr at 298 K was employed; STP states for standard temperature of 273 K and pressure of 760 Torr. The efficiency of photolysis of Cl_2CS is estimated to be ~11% based on its absorption cross section $\sim8\times10^{-18}$ cm^2 $molecule^{-1}$ at 248 nm.[30]

Cl_2CS (95%, Fluka Chemika) and N_2 (99.9995%, AGA Specialty Gases) were used without further purification. CO_2 (99.99%, AGA Specialty Gases) was purified by passing it through a trap with molecular sieve and a trap at 218 K.

III. THEORETICAL CALCULATIONS

The equilibrium geometry, vibrational wave numbers, and IR intensities were calculated with B3P86 and B3LYP density-functional theories using the GAUSSIAN 03 program.[31] The B3LYP method uses Becke's three-parameter hybrid exchange functional with a correlation functional of Lee, Yang, and Parr[32,33] The B3P86 method uses Becke's three-parameter hybrid exchange functional with Perdew's gradient-corrected correlation functional.[34] Dunning's correlation-consistent polarized-valence triple-zeta basis set, augmented with *s*, *p*, *d*, and *f* functions (aug-cc-pVTZ) (Refs. 35 and 36), was applied in these calculations. Analytic first derivatives were utilized in geometry optimization, and vibrational wave numbers were calculated analytically at each stationary point.

The calculated geometry, rotational parameters at the equilibrium geometry, vibrational wave numbers, and IR intensities of ClCS are compared with those of previous workers in Table I. The geometries predicted with various methods are similar. The variations in geometry produce variations of rotational parameters less than 3% for the *A* parameter and 1% for the *B* and *C* parameters, as listed in Table I.

The greater C–S bond length (1.573 Å) calculated with B3LYP/aug-cc-pVTZ is consistent with a smaller wave number (1212 cm^{-1}) predicted for the C–S stretching (ν_1) mode, as compared with values $\nu_1=1314$ cm^{-1} and bond length of 1.565 Å predicted previously with RCISD/6–31G*.[23] Predictions of vibrational wave numbers using B3LYP/aug-cc-pVTZ are estimated to be accurate to within 3%, based on

TABLE I. Comparison of geometry, rotational parameters at equilibrium geometry, vibrational wave numbers, and infrared intensities of ClCS derived from theoretical calculations and experiments.

	RCISD /6-31G*	B3P86 /aug-cc-pVTZ	B3LYP /aug-cc-pVTZ	Ar matrix	Gas
r_{C-S} (Å)	1.565	1.569 [1.589][a]	1.573 [1.573][a]		
r_{C-Cl} (Å)	1.689	1.683 [1.683]	1.697 [1.697]		
∠ClCS (°)	135.8	135.6 [135.6]	135.3 [135.3]		
A (cm^{-1})	4.4461	4.3983 [4.3825]	4.3070 [4.2916]		
B (cm^{-1})	0.1108	0.1113 [0.1083]	0.1101 [0.1072]		
C (cm^{-1})	0.1081	0.1085 [0.1057]	0.1074 [0.1046]		
ν_1 (cm^{-1})	1314	1245.0 (294.1)[b] [1244.6]	1212.4 (289.4)[b] [1212.1]	1189.3	1194.4
ν_2 (cm^{-1})	355	332.7 (1.2) [329.8]	330.0 (1.1) [327.0]		
ν_3 (cm^{-1})	699	655.8 (71.4) [650.5]	630.6 (79.2) [625.6]	632.1	
Reference	23	This work	This work	22	This work

[a]Parameters for ^{37}ClCS are listed in brackets; otherwise values are for ^{35}ClCS.
[b]IR intensities (in km mol^{-1}) are listed in parentheses.

results of similar molecules ClSO (for the S–O stretch, calculated 1156.9 cm^{-1}, gas phase 1162.9 cm^{-1}) (Ref. 26) and ClCO (for the C–O stretch, calculated 1943.5 cm^{-1}, gas phase 1884.6 cm^{-1}).[24] Hence, we expect that the vibrational wave number for the C–S stretching (ν_1) and C–Cl stretching (ν_3) modes to be in the range of 1212±36 and 631±19 cm^{-1}, respectively. The predicted values of ν_1 and ν_3 are near the values of 1189 and 632.1 cm^{-1} reported for matrix-isolated ClCS. Predicted displacement vectors for the C–S stretching mode and the associated dipole derivative are shown in Fig. 1. Wave numbers predicted for Cl–C stretching and ClCS-bending modes are beyond our range of detection.

IV. EXPERIMENTAL RESULTS AND DISCUSSION

Conventional cw absorption measurements were performed with a static cell containing 0.13 Torr of Cl_2CS. The absorption of Cl_2CS is characterized by an intense band near 1137 cm^{-1} (ν_1, C–S stretch).[37] Upon photolysis of the sample at 248 nm (80 mJ, 1 Hz) for 60 s, absorption of CS_2 as the end product is clearly visible near 1529 cm^{-1}.[38] Another band near 2089 cm^{-1} is assigned to the C═S stretching mode (Σ_u^+) of C_3S_2.[39] The mechanism for formation of C_3S_2 will be discussed in the following section. No absorption feature in the static-cell experiment is ascribable to unstable species ClCS or CS.

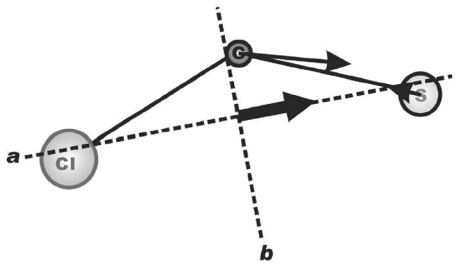

FIG. 1. Rotational axes of ClCS, displacement vectors for the C–S stretching (ν_1) mode, and associated dipole derivative of ClCS predicted with the B3LYP/aug-cc-pVTZ method.

In our previous experiments on ClSO,[26] we found that, at low pressure, the parent was highly internally excited upon laser irradiation, thus producing upward features on each side of the downward parent band in the difference spectrum; in this difference spectrum, features pointing upward indicate increase in concentration, whereas those pointing downward indicate decrease in concentration. We found that these two upward side lobes interfere with nearby absorption bands of dissociation products and hamper their detection. When photolysis was conducted with a sample at high pressure, the upward side lobes diminished and the widths of downward parent features and upward features of product decreased because of efficient relaxation. To quench the internal excitation of Cl_2CS so as to avoid interference due to hot bands, and to stabilize ClCS, we added excessive N_2 or CO_2 in the system; the latter appears to be a more efficient quencher.

A. Spectra of ClCS

A representative three-dimensional plot of temporally resolved survey difference spectra (resolution 4 cm^{-1}) at 2 μs intervals upon laser irradiation at 248 nm of a flowing mixture of Cl_2CS/N_2 (≅1/165, 43 Torr) is shown in Fig. 2. In these difference spectra, features pointing upward indicate production; the downward feature in the range of 1100–1150 cm^{-1} due to loss of Cl_2CS is not shown. Two new features near 1194 and 1285 cm^{-1} appear immediately after irradiation; the former decays with time much more rapidly than the latter. The band near 1285 cm^{-1} is readily assigned to CS,[40] whereas the more intense feature near

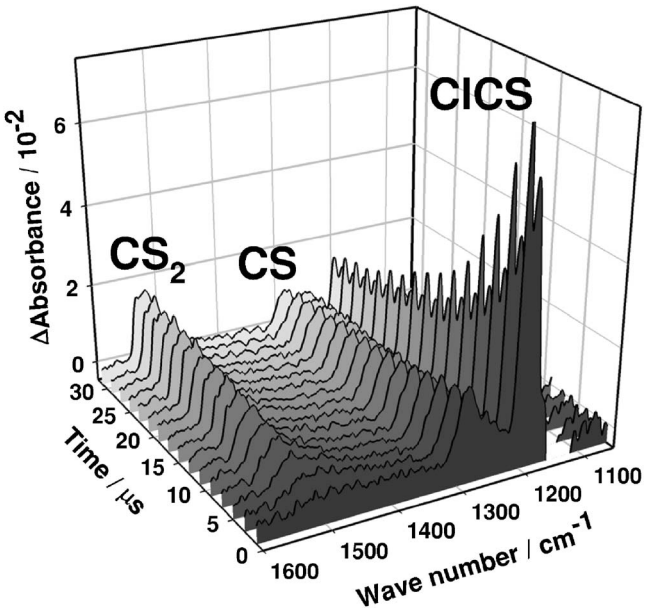

FIG. 2. Time-resolved survey IR absorption spectra of a flowing mixture of Cl_2CS/N_2 upon photolysis at 248 nm (8 Hz, 80 mJ cm^{-2}) displayed in a three-dimensional mode. The flowing mixture is Cl_2CS/N_2 (1/165) at 43 Torr. The path length is 6.4 m and resolution is 4 cm^{-1}. Traces begin 1 μs after irradiation and are separated at 2 μs intervals.

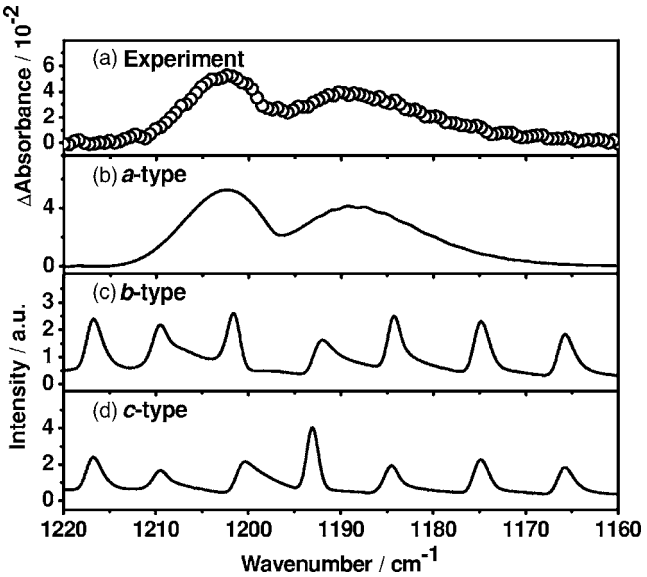

FIG. 3. Comparison of observed and simulated absorption spectra of ClCS. (a) spectrum at resolution of 0.6 cm^{-1} and integrated for 0–20 μs after 248 nm laser irradiation (10 Hz, 80 mJ cm^{-2}) of a flowing mixture of Cl_2CS/CO_2 (1/65) at 52.3 Torr, (b) Simulated *a*-type component based on rotational parameters predicted with B3LYP/aug-cc-pVTZ, (c) *b*-type component, and (d) *c*-type component.

1194 cm^{-1} is new. A third band near 1529 cm^{-1}, attributed to CS_2,[38] appears at a later time, indicating its association with secondary reactions.

Transient absorption spectra in the region of 1160–1220 cm^{-1} with an improved resolution of 0.6 cm^{-1} were recorded upon irradiation of a flowing mixture containing Cl_2CS/CO_2 (1/65) at 52.3 Torr; the spectrum averaged over 0–20 μs after photolysis is shown in trace (a) of Fig. 3. The *P* and *R* branches are clearly distinguishable, but no rotational structure is resolved.

The wave number of the approximate origin of this new feature, 1195 cm^{-1}, is within the expected range of 1212 ± 36 cm^{-1} predicted with the B3LYP/aug-cc-pVTZ method and only slightly greater than the reported value of 1189.3 cm^{-1} for the C–S stretching mode of matrix-isolated ClCS.[22] Considering that this feature appears immediately upon photolysis and decays rapidly due to the great reactivity of its carrier, and that the absorption band of another possible product CS is observed near 1285 cm^{-1}, we tentatively assign this transient absorption to ClCS.

B. Simulation of the ν_1 absorption band of ClCS

As derivation of rotational parameters from observed unresolved spectra is impracticable, we simulate the band contour to compare with observed spectra. Rotational axes *a* and *b* of ClCS are shown in Fig. 1; the *c* axis is perpendicular to the molecular plane. Because the C–S stretching mode alters the dipole moment mainly along the *a* axis, absorption lines for transitions of *a* type are expected to be dominant.

The spectrum at 350 K was simulated (SPECVIEW program[41]) with rotational parameters A'', B'', C'', A', B', and C' derived from quantum-chemical calculations, $J_{max}=120$, and a Gaussian line shape with full width at half-maximum $=0.6$ cm^{-1}. Contributions from ^{37}ClCS are included even though the ^{37}Cl-isotopic shift for the C–S stretching mode is small with a shift of 0.3 cm^{-1} for the origin (Table I) and rotational parameters decreased by 0.4% (A''), 2.7% (B''), and 2.6% (C''), as listed in Table II. Ratios of rotational parameters of the upper ($v_1=1$) and the lower ($v=0$) states (A'/A'', B'/B'', and C'/C'') are calculated to be 0.9727 (0.9722), 0.9956 (0.9958), and 0.9954 (0.9956) with B3LYP/aug-cc-pVTZ (B3P86/aug-cc-pVTZ); these ratios are nearly identical in both methods. Simulated *a*-type, *b*-type, and *c*-type bands are shown in traces (b)–(d) of Fig. 3, respectively. The *a*-type band agrees satisfactorily with experimental observation shown in trace (a), with most characteristic features reproduced. This agreement further supports our assignment of this new feature to the C–S stretching mode of ClCS. The fitting yields a band origin at 1194.4 cm^{-1}, near the value of 1189.3 cm^{-1} reported for the C–S stretching (ν_1) mode of matrix-isolated ClCS.[22]

C. Kinetic behavior of CS, ClCS, and CS_2

One advantage of time-resolved Fourier-transform spectroscopy is its multiplex detection; absorption bands of several species can be monitored concurrently, as illustrated in Fig. 2. The temporal profiles of bands of ClCS (integrated over 1181–1212 cm^{-1}) and CS (integrated over 1235–1325 cm^{-1}) are shown in Figs. 4(a) and 4(b), respectively. Both bands appeared immediately upon photolysis and decayed rapidly with time. The temporal profile of the band due to CS_2, integrated over 1470–1550 cm^{-1} and shown in Fig. 4(c), indicated that this feature appeared at a later stage of reaction.

ClCS and CS are formed initially from direct photolysis,

TABLE II. Comparison of rotational parameters of ^{35}ClCS and ^{37}ClCS predicted with theoretical calculations using B3LYP and B3P86/aug-cc-pVTZ methods.

Parameters		^{35}ClCS		^{37}ClCS	
		B3LYP /aug-cc-pVTZ	B3P86 /aug-cc-pVTZ	B3LYP /aug-cc-pVTZ	B3P86 /aug-cc-pVTZ
$v=0$	A'' (cm^{-1})	4.356 1	4.457 9	4.339 7	4.441 0
	B'' (cm^{-1})	0.109 73	0.110 89	0.106 81	0.107 94
	C'' (cm^{-1})	0.106 79	0.107 96	0.104 01	0.105 16
$v=1$	A' (cm^{-1})	4.237 1	4.333 9	4.220 6	4.317 1
	A'/A''	0.972 7	0.972 2	0.972 6	0.972 1
	B' (cm^{-1})	0.109 24	0.110 43	0.106 34	0.107 50
	B'/B''	0.995 6	0.995 8	0.995 6	0.995 8
	C' (cm^{-1})	0.106 29	0.107 49	0.103 53	0.104 70
	C'/C''	0.995 4	0.995 6	0.995 4	0.995 6

$$Cl_2CS \rightarrow ClCS(X) + Cl(^2P_{3/2}), \quad \Delta H^0 = 265 \text{ kJ mol}^{-1}, \tag{4}$$

$$Cl_2CS \rightarrow Cl_2(X\ ^1\Sigma_g^+) + CS(X\ ^1\Sigma^+), \quad \Delta H^0 = 240 \text{ kJ mol}^{-1}. \tag{5}$$

The energies of the A and B states of ClCS are greater than its ground state by only 77 and 178 kJ mol^{-1}, respectively;[21] hence ClCS was observed to be produced in its A and B states upon photolysis of Cl_2CS at 235 nm.[14] Electronically excited ClCS is expected to relax to its X state within several nanoseconds via radiative processes. We are unable to detect the rapid rise associated with production of ClCS and CS. Subsequent decay of ClCS and CS and formation of CS_2 are results of secondary reactions. Possible secondary reactions include the following reactions involving ClCS and CS radicals and Cl atoms:

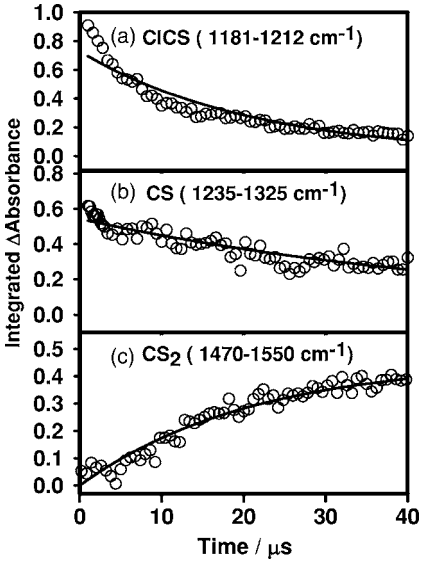

FIG. 4. Temporal profiles of (a) ClCS (integrated over 1181–1212 cm^{-1}), (b) CS (integrated over 1235–1325 cm^{-1}), and (c) CS_2 (integrated over 1470–1550 cm^{-1}) recorded upon 248 nm photolysis of a flowing mixture of Cl_2CS/N_2 (1/165) at 298 K and 43 Torr. Fitted results using first-order kinetics are represented with solid lines; see text.

$$Cl + ClCS \xrightarrow{M} Cl_2CS, \quad \Delta H^0 = -265 \text{ kJ mol}^{-1} \tag{6a}$$

$$\rightarrow Cl_2 + CS, \quad \Delta H^0 = -25 \text{ kJ mol}^{-1}, \tag{6b}$$

$$Cl + CS \xrightarrow{M} ClCS, \quad \Delta H^0 = -215 \text{ kJ mol}^{-1}, \tag{7}$$

$$Cl + Cl \xrightarrow{M} Cl_2, \quad \Delta H^0 = -239 \text{ kJ mol}^{-1}, \tag{8}$$

$$ClCS + ClCS \rightarrow Cl_2CS + CS, \quad \Delta H^0 = -50 \text{ kJ mol}^{-1}, \tag{9}$$

$$CS + CS \xrightarrow{M} C_2S_2, \quad \Delta H^0 = -170 \text{ kJ mol}^{-1}. \tag{10}$$

The exothermicity of reaction (10) is taken from Talbi and Chandler.[42] The reaction

$$CS + ClCS \rightarrow CS_2 + CCl, \quad \Delta H^0 = 157 \text{ kJ mol}^{-1}, \tag{11}$$

is excluded because of its large endothermicity; enthalpies of formation of CS_2 and CCl are 116 ± 1 and 480 ± 20 kJ mol^{-1}, respectively.[19] Reactions (6b) and (9) might be unimportant because of the small exothermicity and because a barrier is expected for the abstraction reaction.

The complicated nature of the reaction mechanism and the lack of measurements of absolute concentrations of Cl, CS, and ClCS preclude accurate modeling of observed temporal profiles. As expected, a simple exponential decay function fit poorly observed decay of ClCS, as shown with the solid line in Fig. 4(a). Based on our proposed mechanism, the consumption reaction of ClCS, mainly reaction (6a), should follow roughly a decay of second-order assuming that initial concentrations of Cl and ClCS upon photolysis are nearly the same and the loss of Cl and ClCS are mainly due to this reaction. For a second-order reaction, the plot of $[ClCS]^{-1}$ versus reaction period t is expected to yield a straight line; the fitting is satisfactory for the first 15 μs, as indicated in Fig. 5(a). The slope of this fitted line is $(1.81 \pm 0.04) \times 10^5$ s^{-1}. If we estimate the initial concentrations of Cl and ClCS to be $\sim 9.2 \times 10^{14}$ molecules cm^{-3} based on absorption cross section of Cl_2CS and laser fluence

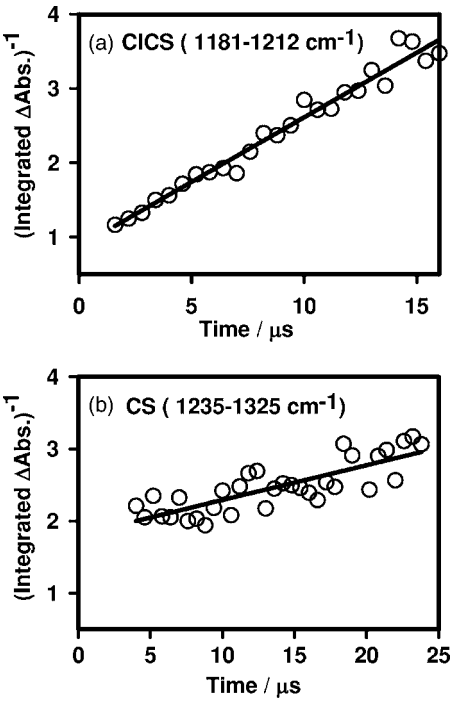

FIG. 5. Plots of (a) $[ClCS]^{-1}$ and (b) $[CS]^{-1}$ vs reaction period t recorded upon 248 nm photolysis of a flowing mixture of Cl_2CS/N_2 (1/165) at 298 K and 43 Torr. Fitted results are represented with solid lines; see text.

at 248 nm, we estimated a rate coefficient $k_6+2k_9 \cong 2.0 \times 10^{-10}$ cm^3 molecule^{-1} s^{-1}. Rate coefficients of k_6 and k_9 have not been reported but are expected to be in the range of $10^{-11}-10^{-10}$ cm^3 molecule^{-1} s^{-1}.

The loss of CS might be mainly due to reactions (7) and (10). At the initial stage, reaction (7) is the most important because the initial concentration of Cl is greater than that of CS, which was initially produced via reaction (2) with a branching ratio of 0.2 ± 0.1.[13] However, the consumption of Cl atoms should be rapid according to reaction (6a) discussed in the previous paragraph. Hence, at the later stage, the temporal profile of CS should follow roughly second-order decay. The plot of $[CS]^{-1}$ versus reaction period t yields a straight line with a slope of $(4.8\pm0.6)\times10^4$ s^{-1} in the range of 5–25 μs, as shown in Fig. 5(b). However, we did not observe transient absorption of C_2S_2 at 1180 cm^{-1} partly because of its small concentration and partly because of overlap of this band with nearby absorption band of ClCS.[43]

A single exponential rise with a pseudo-first-order rate coefficient of $(4.8\pm0.3)\times10^4$ s^{-1} fits satisfactorily observed generation of CS_2, as shown in Fig. 4(c). The generation of CS_2 might be due to the reaction of C_2S_2 and CS,

$$C_2S_2 + CS \rightarrow C_2S + CS_2, \quad \Delta H^0 = 47 \text{ kJ mol}^{-1}, \qquad (12)$$

in which enthalpies of formation of C_2S at 0 K is 586 kJ mol^{-1};[44] the small endothermicity may be compensated by the exothermicity of reaction (10). It is also possible that the reaction of CS+S also contributes to the formation of CS_2; S atoms might be produced upon photolysis of S_2Cl_2, the most abundant impurity in the sample of Cl_2CS. Further reaction of C_2S, produced in reaction (12), with CS produces stable C_3S_2,[43]

$$C_2S + CS \rightarrow C_3S_2. \qquad (13)$$

This might explain the observation of a small amount of C_3S_2 in the static-cell experiment; the IR absorption cross section of C_3S_2 at 2089 cm^{-1} is predicted to be 3160 km mol^{-1}, five times greater than that of the C–S antisymmetric stretching band of CS_2 at 1529 cm^{-1}.

V. CONCLUSION

We demonstrate an application of the time-resolved Fourier-transform absorption technique to detect a transient absorption band at 1194.4 cm^{-1}, ascribed to the C–S stretching mode of ClCS produced upon photolysis of gaseous Cl_2CS. The rotational contour of the observed spectrum conforms satisfactorily to a simulated *a*-type spectrum based on rotational parameters predicted from quantum-chemical calculations; the vibrational wave number is consistent with that predicted for the C–S stretching mode of ClCS. The formation and decay of ClCS, CS, and CS_2 were recorded, and the associated reaction mechanism is discussed.

ACKNOWLEDGMENTS

The authors thank V. Stakhursky and T. A. Miller for providing the SPECVIEW software for spectral simulation, the National Center for High-Performance Computing of Taiwan for computer facilities, the National Science Council of Taiwan (Grant No. NSC95-2119-M-009-032), and the MOE-ATU Program for support.

[1] N. J. Turro, V. Ramamurthy, W. Cherry, and W. Farneth, Chem. Rev. (Washington, D.C.) **78**, 125 (1978).
[2] R. P. Steer, Rev. Chem. Intermed. **4**, 1 (1981), and references therein.
[3] A. Maciejewski and R. P. Steer, Chem. Rev. (Washington, D.C.) **93**, 67 (1993), and references therein.
[4] D. J. Clouthier and D. C. Moule, Top. Curr. Chem. **150**, 167 (1989).
[5] H. Morrison, Y. Lu, and D. Carlson, J. Phys. Chem. A **102**, 5421 (1998).
[6] H. Okabe, J. Chem. Phys. **66**, 2058 (1977).
[7] D. C. Moule, I. R. Burling, H. Liu, and E. C. Lim, J. Chem. Phys. **111**, 5027 (1999).
[8] T. Fujiwara, D. C. Moule, and E. C. Lim, J. Phys. Chem. A **107**, 10223 (2003).
[9] R. H. Judge and D. C. Moule, J. Mol. Spectrosc. **80**, 363 (1980).
[10] R. N. Dixon and C. M. Western, J. Mol. Spectrosc. **115**, 74 (1986).
[11] M. Ludwiczak, D. R. Latimer, and R. P. Steer, J. Mol. Spectrosc. **147**, 414 (1991).
[12] B. Simard, V. J. MacKenzie, P. A. Hackett, and R. P. Steer, Can. J. Chem. **72**, 745 (1994).
[13] G. S. Ondrey and R. Bersohn, J. Chem. Phys. **79**, 175 (1983).
[14] T. S. Einfeld, C. Maul, K.-H. Gericke, and A. Chichinin, J. Chem. Phys. **117**, 1123 (2002).
[15] A. Kapur, R. P. Steer, and P. G. Mezey, J. Chem. Phys. **70**, 745 (1979).
[16] B. Simard, A. E. Bruno, P. G. Mezey, and R. P. Steer, Chem. Phys. **103**, 75 (1986).
[17] B. Strickler and M. Gruebele, Chem. Phys. Lett. **349**, 137 (2001).
[18] L. Lin, F. Zhang, W.-J. Ding, W.-H. Fang, and R.-Z. Liu, J. Phys. Chem. A **109**, 554 (2005).
[19] M. W. Chase, Jr., J. Phys. Chem. Ref. Data Monogr. **9**, 1 (1998).
[20] D. A. Prinslow and P. B. Armentrout, J. Chem. Phys. **94**, 3563 (1991).
[21] M. Hachey, F. Grein, and R. P. Steer, Can. J. Chem. **71**, 112 (1993).
[22] G. Schallmoser, B. E. Wurfel, A. Thoma, N. Caspary, and V. E. Bondybey, Chem. Phys. Lett. **201**, 528 (1993).
[23] W.-T. Chan and J. D. Goddard, Chem. Phys. Lett. **173**, 139 (1990).
[24] S.-H. Chen, L.-K. Chu, Y.-J. Chen, I-C. Chen, and Y.-P. Lee, Chem. Phys. Lett. **333**, 365 (2001).
[25] Y.-J. Chen, L.-K. Chu, S.-R. Lin, and Y.-P. Lee, J. Chem. Phys. **115**, 6513 (2001).

[26] L.-K. Chu, Y.-P. Lee, and E. Y. Jiang, J. Chem. Phys. **120**, 3179 (2004).
[27] L.-K. Chu and Y.-P. Lee, J. Chem. Phys. **124**, 244301 (2006).
[28] W. Uhmann, A. Becker, C. Taran, and F. Siebert, Appl. Spectrosc. **45**, 390 (1991).
[29] E. Y. Jiang, Spectroscopy (Eugene, Or.) **17**, 22 (2002).
[30] E. R. Farnsworth and G. W. King, J. Mol. Spectrosc. **46**, 419 (1973).
[31] M. J. Frisch, G. W. Trucks, H. B. Schlegel *et al.*, GAUSSIAN 03, Revision A.7, Gaussian, Inc., Pittsburgh, PA, 1998.
[32] A. D. Becke, J. Chem. Phys. **98**, 5648 (1993).
[33] C. Lee, W. Yang, and R. G. Parr, Phys. Rev. B **37**, 785 (1988).
[34] J. P. Perdew, Phys. Rev. B **33**, 8822 (1986).
[35] T. H. Dunning, Jr., J. Chem. Phys. **90**, 1007 (1989).
[36] D. E. Woon and T. H. Dunning, Jr., J. Chem. Phys. **98**, 1358 (1993).
[37] T. Shimanouchi, J. Phys. Chem. Ref. Data **6**, 993 (1977).
[38] T. Shimanouchi, *Tables of Molecular Vibrational Frequencies. Consolidated Volume I* (National Bureau of Standards, Gaithersburg, MD, 1972).
[39] Wm. H. Smith and G. E. Leroi, J. Chem. Phys. **45**, 1778 (1966).
[40] G. Herzberg, *Molecular Spectra and Molecular Structure. I. Spectra of Diatomic Molecules* (Van Nostrand Reinhold, New York, 1950).
[41] V. Stakhursky, T. A. Miller, 56th OSU International Symposium on Molecular Spectroscopy, Columbus, Ohio, 2001 (unpublished); SPECTVIEW: Simulation and Fitting of Rotational Structure of Electronic and Vibronic Bands, http://www.chemistry.ohio-state.edu/~vstakhur
[42] D. Talbi and G. S. Chandler, J. Phys. Chem. A **104**, 5872 (2000).
[43] R. B. Bohn, Y. Hannachi, and L. Andrews, J. Am. Chem. Soc. **114**, 6452 (1992).
[44] Y. H. Le Teuff, T. J. Millar, and A. J. Markwick, Astron. Astrophys., Suppl. Ser. **146**, 157 (2000).